Behavioral/Systems/Cognitive

A Specific Limbic Circuit Underlies Opiate Withdrawal Memories

François Frenois,[1] Luis Stinus,[1] Francesco Di Blasi,[2] Martine Cador,[1]* and Catherine Le Moine[1]*

[1]Centre National de la Recherche Scientifique Unité Mixte de Recherche 5541 "Interactions Neuronales et Comportements," Université Victor Segalen Bordeaux 2, 33076 Bordeaux cedex, France, and [2]Institut National de la Santé et de la Recherche Médicale Unité 588 "Physiopathologie du Comportement," Université Victor Segalen Bordeaux 2, Institut François Magendie, 33077 Bordeaux cedex, France

Compulsive drug-seeking behavior and its renewal in former drug addicts is promoted by several situations, among which reactivation of drug withdrawal memories plays a crucial role. A neural hypothesis is that such memories reactivate the circuits involved in withdrawal itself and promote a motivational state leading to drug seeking or taking. To test this hypothesis, we have analyzed the neural circuits and cell populations recruited when opiate-dependent rats are reexposed to stimuli previously paired with withdrawal (memory retrieval) and compared them with those underlying acute withdrawal during conditioning (memory formation). Using *in situ* hybridization for c-*fos* expression, we report here that reexposure to a withdrawal-paired environment induced conditioned c-*fos* responses in a specific limbic circuit, which can be partially dissociated from the structures involved in acute withdrawal. At the amygdala level, c-*fos* responses were doubly dissociated between the central and basolateral (BLA) nuclei, when comparing the two situations. Detailed phenotypical analyses in the amygdala and ventral tegmental area (VTA) show that specific subpopulations in the BLA are differentially involved in the formation and retrieval of withdrawal memories, and strikingly that a population of VTA dopamine neurons is activated in both situations. Together, this indicates that withdrawal memories can drive activity changes in specific neuronal populations of interconnected limbic areas known to be involved in aversive motivational processes. This first study on the neural substrates of withdrawal memories strongly supports an incentive–motivational view of withdrawal in opiate addiction that could be crucial in compulsive drug seeking and relapse.

Key words: conditioned stimuli; c-*fos* imaging; rat brain; extended amygdala; dopamine; incentive learning

Introduction

Although the first stage of opiate addiction is linked to the intrinsic reinforcing effects of the drug, the development of compulsive drug seeking may be additionally motivated by the appearance of dependence and avoidance of withdrawal aversion. Hence, in former addicts, even the sole memory of withdrawal can generate a motivational state leading to renewed drug taking. Such memories can be reactivated by contexts or situations previously associated with drug taking or drug withdrawal (Wikler, 1973; Childress et al., 1993). At a neural level, it has been proposed that, through conditioning, such environments acquire the ability to activate the circuits involved in the drug effects or withdrawal and therefore reinstate drug-seeking motivation (Stewart et al., 1984; Self and Nestler, 1998; Koob and Le Moal, 2001). We have recently described a specific limbic network [including the amyg-

dala and ventral tegmental area (VTA)] as a key complex for the aversive aspect of opiate withdrawal that is partially dissociated from the brain sites involved in its somatic aspect (Frenois et al., 2002). To better characterize the motivational component of opiate withdrawal and the trace of its memory in the brain, we have compared the neural pathways recruited during the formation and retrieval of withdrawal memories by using a conditioned place aversion paradigm. The conditioning protocol that we used allowed us to dissociate the respective role played by proximal cues (the sensory cues provided by the compartments of the place aversion apparatus) and distal cues provided by the environmental context (the room in which the apparatus was located). We have analyzed and quantified c-*fos* mRNA expression in the rat brain by extensive *in situ* hybridization after acute withdrawal and reexposure to withdrawal-paired stimuli, then we have characterized at a cellular level the populations involved within specific areas of interest.

Materials and Methods

Animals and treatments

Sprague Dawley male rats (IFFA-CREDO, Lyon, France) weighing 180–200 g were housed in standard conditions as described by Frenois et al. (2002). Rats were handled for 10 d before the beginning of the experiments (all conducted during the light cycle). All procedures were performed in accordance with the European Directive (86/609/EEC) and with the French Centre National de la Recherche Scientifique approval.

Table 1. Experimental design for opiate withdrawal conditioning

Morphine-dependent groups	n	Conditioning phase				Test phase (behavior)	Confinement (c-fos)
		Y-maze room (ENV+)		Colony room (ENV−)		Y-maze room (ENV+)	Y-maze room (ENV+)
		cs− (days 5, 7, 9)	cs+ (days 6, 8, 10)	Home cage (days 6, 8, 10)		Day 11, 20 min	Day 13, 60 min
Ct	6	Saline	Saline	Saline		Free exploration of the entire Y-maze	Random
ENV−	6	Saline	Saline	Naloxone (120 μg/kg)		Free exploration of the entire Y-maze	Random
ENV+ (ENV+/cs+)	8	Saline	Naloxone (120 μg/kg)	Saline		Free exploration of the entire Y-maze	cs+
ENV+ (ENV+/cs−)	8	Saline	Naloxone (120 μg/kg)	Saline		Free exploration of the entire Y-maze	cs−

Ct, Control (no opiate withdrawal); ENV−, group with opiate withdrawal negatively paired with the Y-maze room context during conditioning. Instead, withdrawal was precipitated by naloxone in the colony room; ENV+/cs+ and ENV+/cs−, groups with naloxone-precipitated withdrawal positively paired with the Y-maze room context (conditioning environment) during the conditioning phase. On day 11, rats explored the entire Y-maze for 20 min to measure a place aversion score (behavioral test). On day 13, rats were reexposed to the conditioning environment (ENV+) for 60 min before decapitation for c-fos study in a specific compartment of the Y-maze (cs+ or cs−) depending on their group assignment.

Morphine dependence was induced by subcutaneous implantation of two slow-release morphine-containing pellets (75 mg of morphine base each; National Institute on Drug Abuse, Bethesda, MD), under anesthesia (halothane/O$_2$; induction 4:100 v/v for 10 s, followed by 1.5:100 v/v for 30 s), and all of the animals were implanted with morphine pellets. Full dependence on morphine has been previously operationally defined in this model by using a complete naloxone dose effect on various behavioral parameters (spontaneous locomotor activity, operant responding for food, intracranial self-stimulation threshold, conditioned place aversion) (Schulteis et al., 1994), and the rating of abstinence signs showed that opiate dependence was achieved 24 h after implantation of the morphine pellets and remained constant for 15 d (Gold et al., 1994). Morphine withdrawal was precipitated by subcutaneous injections of 120 μg/kg naloxone hydrochloride (RBI/Sigma-Aldrich, Saint Quentin Fallavier, France) dissolved in isotonic saline (the naloxone dose was expressed as free base, 1 mg of naloxone base = 1.113 mg of naloxone hydrochloride). Note that this naloxone dose has previously been shown to be without effect on both place aversion conditioning and Fos expression in placebo control rats (Gestreau et al., 2000; Hamlin et al., 2001; Frenois et al., 2002).

Conditioned place aversion and experimental design
The experimental design is described in detail in supplemental Figure 1 (available at www.jneurosci.org as supplemental material). Conditioned place aversion took place in an unbiased Y-maze, as described previously by Caillé et al. (1999), that comprised three compartments differentiated by visual and tactile cues, which are readily discriminated by rats. In the preconditioning phase (4 d after morphine pellet implantation), rats were allowed to freely explore the apparatus for 20 min. Rats showing strong unconditioned aversion or preference for any compartment were discarded (i.e., <17% and >48% of the session time, respectively). For each rat, the two compartments with the closest time allotments were chosen, and one was randomly paired with naloxone and the other was randomly paired with saline, as described previously by Caillé et al. (1999). After compartment assignment, *post hoc* Dunn's multiple comparisons test showed that there was no difference between the time spent in the naloxone-paired (cs+; 431.1 ± 10.2 s) and the saline-paired (cs−; 443.3 ± 10.7 s) compartments during the preconditioning phase but that these two Y-maze compartments were both different from the third (neutral) compartment (325.8 ± 9.1 s; p < 0.001 in both cases; Kruskal–Wallis test; p < 0.0001). During the conditioning phase (three sessions that started on day 5 after morphine pellet implantation), rats were confined in one compartment of the Y-maze for 20 min (Table 1): rats in group ENV+ received a saline injection before being placed in the cs− compartment on days 5, 7, and 9 after pellet implantation, and on alternate days (6, 8, and 10), they received a naloxone injection (120 μg/kg to precipitate morphine withdrawal) before being placed in the cs+ compartment. To isolate responses induced by contextual stimuli (i.e., the room in which the Y-maze was placed), rats in group ENV− received saline injections in both Y-maze compartments but experienced with-

drawal in the colony room on days 6, 8, and 10, whereas ENV+ rats received saline injections in this latter context. A control (Ct) group received only saline injections (in the two Y-maze compartments and in the colony room). All rats were therefore equated in the number of exposures to environments and injections. The behavioral testing phase was aimed to control for conditioning effectiveness and consisted of a free exploration of the entire Y-maze for 20 min on day 11 after pellet implantation, during which the time spent in each compartment was recorded. A place aversion score was calculated as the difference between the times spent in the same compartment during the testing phase and the preconditioning phase. Statistical analysis was performed using the Wilcoxon matched-pairs test.

To study the neural pathways involved in the retrieval of withdrawal memories (measured by conditioned c-fos expression), all rats were confined for 60 min in a specific Y-maze compartment on day 13 after pellet implantation before being killed by decapitation. Note that during reexposure, rats are not allowed to have control over their behavior and that this procedure specifically tests the retrieval of an emotional aversive state generated by previous opiate withdrawal episodes and not the behavioral consequence of this memory (e.g., conditioned place aversion). The ENV+ group was split into two subgroups: rats in group ENV+/cs+ were reexposed to the cs+ compartment, whereas rats in group ENV+/cs− were reexposed to the cs− compartment. Ct and ENV− rats were randomly reexposed to one of the two compartments. This experimental procedure allows us to compare the relative weight of two sets of withdrawal-paired environmental stimuli on conditioned c-fos responses: the influence of the proximal set of stimuli (features of the Y-maze compartments) can be assessed by the comparison between the ENV+/cs+ and ENV+/cs− groups, and the influence of the distal set of stimuli (environmental context) can be assessed by the comparison between the ENV+ and ENV− groups. To compare the conditioned c-fos responses with the acute effects of morphine withdrawal during memory formation, two other groups were used: 120 μg/kg naloxone (Nal120; n = 8) and saline (Sal; n = 8). These rats were handled in the same conditions as the ENV+, ENV−, and Ct rats until the end of the first conditioning session (on day 6), during which Nal120 rats experienced acute naloxone-precipitated withdrawal, whereas Sal rats received a saline injection. Then, after a 60 min period of confinement in one compartment of the Y-maze, rats were killed by decapitation.

In situ *hybridization*
Immediately after decapitation, brains were dissected out and frozen into vapors of liquid nitrogen. Serial coronal cryostat sections (12 μm thick) were then collected on gelatin-coated slides and stored at −80°C.
Construction of tyrosine hydroxylase cDNA. A 600 bp fragment corresponding to nucleotides 1021–1620 of the rat tyrosine hydroxylase (TH) gene (National Center for Biotechnology Information gene bank accession number M10244) was generated by reverse transcription-PCR on poly(A)$^+$ RNA isolated from total rat brain RNA. After reverse transcription using PowerScript RT (Clontech, Palo Alto, CA), 100 ng of

Table 2. c-*fos* mRNA levels after acute morphine withdrawal and reexposure to withdrawal-paired environments

Brain areas (distance from bregma)	Acute withdrawal		Conditioned situation			
	Sal (n = 8)	Nal120 (n = 8)	ENV+/cs+ (n = 8)	ENV+/cs− (n = 8)	ENV− (n = 6)	Ct (n = 6)
Macroscopic analysis						
Prelimbic cortex (+3.70 mm)	1269 ± 104	2137 ± 409	1331 ± 228	1266 ± 94	1086 ± 142	1101 ± 149
Cingulate cortex (+1.20 mm)	536 ± 69	831 ± 116*	510 ± 95	471 ± 74	392 ± 70	430 ± 79
Primary motor cortex (+1.20 mm)	468 ± 60	880 ± 149*	358 ± 21	329 ± 12	311 ± 12	323 ± 20
Primary somatosensory cortex (+1.20 mm)	377 ± 31	566 ± 69*	231 ± 16	247 ± 17	224 ± 15	250 ± 33
Caudate putamen						
Dorsomedial part (+1.20 mm)	206 ± 31	412 ± 75*	171 ± 11	164 ± 5	156 ± 9	165 ± 11
Ventromedial part (+1.20 mm)	183 ± 23	428 ± 74*	172 ± 13	167 ± 3	156 ± 11	172 ± 8
Dorsolateral part (+1.20 mm)	186 ± 21	275 ± 40	174 ± 11	163 ± 8	155 ± 10	158 ± 10
Ventrolateral part (+1.20 mm)	162 ± 20	227 ± 31	166 ± 9	160 ± 6	149 ± 9	164 ± 12
Lateral septal nucleus (0.26 mm)	241 ± 36	1019 ± 114***	173 ± 8	210 ± 16	206 ± 8	213 ± 13
Microscopic analysis						
Acb						
Core (+1.20 mm)	33 ± 3	90 ± 5***	71 ± 5	82 ± 5	66 ± 7	62 ± 6
Shell medial part (+1.20 mm)	61 ± 8	328 ± 27***	202 ± 21***^^^	198 ± 21***^^^	74 ± 9	90 ± 16
BNST						
Dorsal part (−0.26 mm)	118 ± 9	631 ± 70***	144 ± 11***^^^	170 ± 9***^^^	71 ± 10	66 ± 4
Ventral part (−0.26 mm)	108 ± 11	654 ± 61***	251 ± 22***^^^	246 ± 30***^^^	80 ± 15	82 ± 9
Amygdala						
BLA (−2.12 mm)	144 ± 8	104 ± 14*	186 ± 17**^^	175 ± 12**^^	106 ± 9	102 ± 12
CeA (−2.12 mm)	87 ± 8	491 ± 44***	69 ± 10*	73 ± 9*	95 ± 9	117 ± 16
Hypothalamic nuclei						
Lateral (−2.12 mm)	94 ± 14	279 ± 27***	117 ± 12^	122 ± 11^	79 ± 10	88 ± 11
PVH (−2.12 mm)	167 ± 31	1229 ± 86***	376 ± 60***^^	380 ± 69**^^	80 ± 7	73 ± 8
VTA (−5.30 mm)	33 ± 4	119 ± 9***	106 ± 8***^^^	112 ± 13***^^^	30 ± 4	38 ± 5
Periaqueductal gray (−5.30 mm)	114 ± 9	197 ± 19**	108 ± 4	108 ± 11	100 ± 6	94 ± 8
Hippocampus						
CA1 hippocampic field (−5.30 mm)	75 ± 8	333 ± 36***	156 ± 30*^	149 ± 16*^	75 ± 7	74 ± 3
CA3 hippocampic field (−5.30 mm)	63 ± 6	218 ± 21***	128 ± 8***^^^	115 ± 11**^^	70 ± 6	67 ± 5
LC (−10.04 mm)	55 ± 10	718 ± 27***	294 ± 55***^^^	313 ± 42***^^^	40 ± 8	38 ± 7
Nucleus of the solitary tract (−13.24 mm)	183 ± 10	459 ± 57***	205 ± 20	205 ± 23	184 ± 17	184 ± 18

Twenty-three brain areas were measured at various levels from bregma (Paxinos and Watson, 1997). Densitometry was chosen for areas that can be delineated on X-ray films on basal conditions (lateral septal nucleus, caudate putamen, and cortical areas). For other structures, cellular analysis was chosen for required accurate delineation. Values represent mean ± SEM of arbitrary units of radioactivity for densitometry and of the density of c-*fos* + neurons per millimeter squared for the cellular analysis. Statistics were performed by unpaired *t* tests in the acute withdrawal situation (*$p < 0.05$, ***$p < 0.001$ vs saline group) and by ANOVA and *post hoc* Newman–Keuls test for the conditioned situation (*$p < 0.05$, **$p < 0.01$, ***$p < 0.001$ vs Ct group; ^$p < 0.05$, ^^$p < 0.01$, ^^^$p < 0.001$ vs ENV− group).

cDNA was used for PCR. PCR was performed with oligo-specific primers (forward, 5′-tacccatgttggctgaccgcacatttg-3′; reverse, 5′-catcaaagggccca-gccacacacatgg-3′) with GoldStar *Taq* polymerase (Eurogentec, Liege, Belgium) and cloned into pBluescript II SK (Stratagene, La Jolla, CA). The resulting construct was confirmed by DNA sequencing.

Probe synthesis and labeling for in situ *hybridization.* The c-*fos* probe (Curran et al., 1987) was labeled by *in vitro* transcription with ^{35}S-UTP (>1000 Ci/mmol; PerkinElmer Life Sciences, Courtaboeuf, France), whereas the TH (PCR product) and GAD67 (isoform 67 of the glutamic acid decarboxylase) (Julien et al., 1987) probes were labeled with digoxigenin-11-UTP (Roche Diagnostics, Meylan, France) using appropriate T3, T7, or SP6 RNA polymerases (Promega, Charbonnières, France) and purified as described by Frenois et al. (2002).

In situ *hybridization experiments.* Experiments were performed as described by Frenois et al. (2002). Briefly, sections were hybridized overnight at 55°C with 10[6] cpm of ^{35}S-labeled c-*fos* probe (for single labeling) or a combination of 10[6] cpm of ^{35}S-labeled c-*fos* probe with 10–20 ng of digoxigenin-labeled TH or GAD67 probes (for double labeling). Slides were rinsed, treated with RNase A, washed in decreasing SSC concentrations at room temperature and then at 65°C, and dehydrated. For single labeling, sections were then dipped into Ilford K5 emulsion, dried, and apposed to Biomax MR X-ray films (Eastman Kodak, Rochester, NY) for 1 month. Sections were developed and fixed after 3 months of exposure in the dark before counterstaining. For double labeling, sections were processed as described by Svenningsson et al. (2000). Briefly, after incubation with alkaline phosphatase-conjugated anti-digoxigenin antibody (1:1000; Roche Diagnostics), sections were dipped into Ilford K5 emulsion and exposed for 3 months in the dark. Sections were then developed and fixed, rinsed, and incubated overnight in the dark into the alkaline phosphatase substrate (5-bromo-4-chloro-3-indolyl phosphate/nitroblue tetrazolium). After rinsing, sections were mounted in Eukitt.

Data analysis. c-*fos* mRNA levels were quantified by densitometry or cellular counting depending on the structures examined, as described by Frenois et al. (2002), with an image analyzer (Densirag 200 and VisioScan 200; Biocom, Paris, France). Optical densities or the number of c-*fos*+ neurons per millimeter squared were averaged for each group. For the cellular analysis, c-*fos*+ neurons were divided into TH+ and TH− neurons in the VTA and into GAD+ and GAD− neurons in the basolateral amygdala (BLA). Statistical analyses were performed by ANOVA, followed by the *post hoc* Newman–Keuls multiple comparisons test for the Ct, ENV−, ENV+/cs+, and ENV+/cs− groups, and by unpaired *t* tests to compare acute withdrawal (Nal120 group) to control (Sal group). Values are expressed as mean ± SEM. In the BLA, grain densities were measured as described by Svenningsson et al. (2000) in c-*fos*+/GAD+ and c-*fos*+/GAD− neurons for the Sal and Nal120 groups. Frequency distributions of grain densities were plotted for both groups and compared by a Kolmogorov–Smirnov test. Nonparametric Mann–Whitney *U* tests were used to compare the medians of grain densities between groups.

Results

The conditioned c-*fos* responses are driven by the entire environmental context

The animal's reexposure to withdrawal-paired environmental stimuli induced significant c-*fos* variations in a set of interconnected limbic areas (extended amygdala, BLA, hippocampus, and VTA), as well as in the locus ceruleus (LC) and paraventricular hypothalamus (PVH) (Table 2). A main statistical effect across the conditioned groups indicated that the ENV+ rats showed variations of c-*fos* mRNA versus Ct and ENV− rats, but no difference neither between ENV+/cs+ and ENV+/cs− nor between Ct and ENV− rats was observed (Table 2). As mentioned
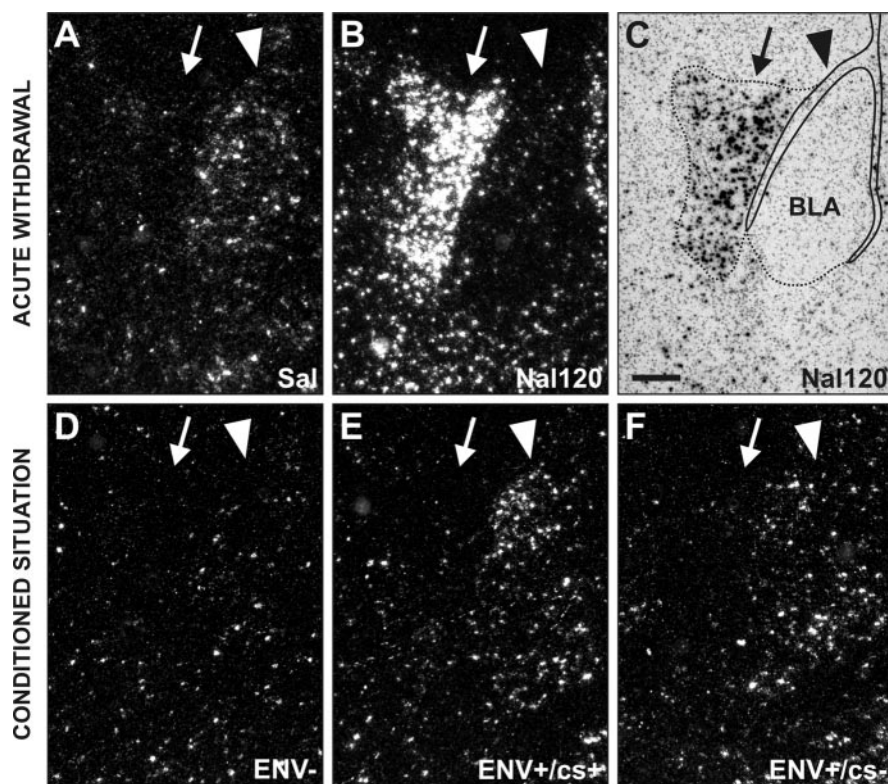
Figure 1. Conditioned c-*fos* responses and withdrawal-induced c-*fos* expression in the CeA and BLA. Dark-field micrographs show labeling within the amygdala in the acute withdrawal (*A, B*) and conditioned (*D–F*) situations. Arrowheads point to the BLA, and arrows point to the CeA. *C*, Bright-field micrograph of the section shown in *B* delineating areas of quantification. In the Sal group, c-*fos* basal levels were higher in the BLA than in the CeA (*A*), whereas no difference was observed between the CeA and BLA in ENV− animals (*D*). Acute withdrawal increases c-*fos* mRNA in the CeA but decreases it in the BLA (*B*). Conversely, both ENV+/cs+ (*E*) and ENV+/cs− (*F*) rats showed similar conditioned c-*fos* increases in the BLA after reexposure to the Y-maze environment. In contrast, the levels of c-*fos* mRNA are decreased in the CeA for conditioned animals (ENV+/cs+ and ENV+/cs−). Scale bar, 500 μm.

in Materials and Methods, our experimental procedure was designed to map the memory trace of the negative affective state generated by previous morphine withdrawal episodes, which can be induced by different kinds of environmental stimuli (ENV+ vs ENV− for distal environmental contexts and cs+ vs cs− for proximal stimuli) (Table 1 and supplemental Fig. 1, available at www.jneurosci.org as supplemental material). In all of the brain sites analyzed, there was no c-*fos* variation in rats withdrawn in the colony room but reexposed to the Y-maze (ENV− group) that were at control levels, and conditioned c-*fos* responses were detected after reexposure to the Y-maze room context (ENV+) regardless of the specific Y-maze compartment (cs+ or cs−) used for confinement (Tables 1, 2). These data show that the conditioned c-*fos* responses induced by reexposure to withdrawal-paired stimuli are preferentially driven by a conditioning to the entire environmental context.

Role of the proximal and distal sets of withdrawal-paired stimuli
During the behavioral control phase, rats were allowed to freely explore the entire Y-maze for 20 min (see Materials and Methods). The results show that all ENV+ animals massively avoided their naloxone-paired compartment (mean ± SEM of the aversion score for the cs+ compartment = −289.9 ± 23.0 s; Wilcoxon matched-pairs test; $p = 0.0005$), indicating a transfer of

the aversive properties of previous withdrawal episodes to the cs+ compartment. Examination of the avoidance strategy shows that ENV+ rats divided their activity between the cs− compartment and the neutral compartment (mean ± SEM of the behavioral scores for the cs− and neutral compartments = 128.0 ± 39.2 s and 161.9 ± 35.3 s, respectively). These results indicate that there was no preference for the cs− compartment compared with the neutral one and therefore that the cs− compartment did not acquire full "safe" properties through conditioning. However, although ENV+ animals did avoid the cs+ compartment when given the choice, we observed in our mapping analysis a similar pattern of c-*fos* gene expression after reexposure in either the cs+ or cs− compartment. In this latter situation, rats were confined in a given compartment and were not able to have control over their behavior. Together, these data show that, during conditioning, rats can associate both the proximal (cs+ compartment features) and the distal (Y-maze room features) sets of stimuli with morphine withdrawal, which are both later on able to influence brain reactivity and behavior, depending on the experimental situation (free choice vs reexposure).

Comparison of conditioned c-*fos* responses with the acute withdrawal effects
Quantification of c-*fos* mRNA levels (Table 2) showed that acute withdrawal modified c-*fos* expression in a large set of structures that is in total agreement with Frenois et al. (2002) but that reexposure to withdrawal-paired environmental stimuli induced c-*fos* expression variations only in a subset of these many areas, which is composed of specific interconnected limbic structures (extended amygdala, BLA, hippocampus, and VTA) and the LC and PVH. Thus, the changes in the activity of these brain sites (generated by conditioned stimuli), which represent specifically the retrieval of an emotional aversive state previously associated with morphine withdrawal, can be dissociated from the acute withdrawal effect.

In most structures analyzed, the conditioned c-*fos* responses were globally lower than the acute withdrawal effects (Table 2). However, particular patterns were found in the amygdala and VTA. In the amygdala, reexposure to withdrawal-paired stimuli induced c-*fos* expression in the BLA (+75% for ENV+/cs+, +65% for ENV+/cs−) but inhibited it in the central amygdala (CeA) (−41% for ENV+/cs+, −38% for ENV+/cs−). Note that the results were identical between the ENV+/cs+ and ENV+/cs− groups when quantifying separately the lateral part and the basal part of the BLA complex (data not shown). Conversely, acute withdrawal strongly increased c-*fos* mRNA expression in the CeA (+464%) but decreased it in the BLA (−28%). Together, these data show a double dissociation between the CeA and BLA in c-*fos* expression (Fig. 1). In the VTA, c-*fos* mRNA was strongly increased, and strikingly, to a similar extent after acute with-

drawal (+261%) and reexposure to withdrawal-paired stimuli (+253% for ENV+/cs+, +273% for ENV+/cs−).

Specific opposite c-*fos* responses within the amygdala

The BLA mainly contains glutamate output neurons (GAD−) together with GABA interneurons (GAD+), and the CeA contains only GAD+ neurons. Because a double dissociation was found in the BLA and CeA (Table 2, Fig. 1), a phenotypic analysis was performed to characterize the neuronal populations involved to better understand the cellular events underlying these processes. Double-labeling showed that acute withdrawal decreased the density of c-*fos*+/GAD− neurons (−67%) (Figs. 2A, 3A,B), whereas reexposure to withdrawal-paired stimuli increased it (+95% for ENV+/cs+, +67% for ENV+/cs−) (Figs. 2B, 3C,D), with no significant effect on the density of c-*fos*+/GAD+ neurons. In the CeA, we showed a +1229% increase in c-*fos*+/GAD+ neurons after acute withdrawal (Fig. 2C), and, in contrast, reexposure to withdrawal-paired stimuli significantly decreased the number of c-*fos*+/GAD+ neurons versus ENV− rats (−25% for ENV+/cs+, −24% for ENV+/cs−) (Fig. 2D).

A subpopulation of BLA output neurons is activated by acute opiate withdrawal

In the BLA, despite a global decrease in the number of c-*fos*+ neurons after acute withdrawal, we noticed that the remaining labeled neurons expressed very high c-*fos* mRNA levels (Fig. 3A,B). Thus, grain densities were measured in c-*fos*+ neurons for the Nal120 and Sal groups, and frequency distributions for c-*fos*+/GAD− (Fig. 4A) and c-*fos*+/GAD+ (Fig. 4B) were plotted. In the Sal group, 562 GAD− neurons exhibited c-*fos* labeling (Fig. 4A, light histogram), whereas only 231 GAD− neurons were labeled after acute withdrawal (Fig. 4A, dark histogram). However, the median of grain density in the remaining labeled neurons (Fig. 4A, inset) was increased (39.6 vs 14.6 in the Sal group). This indicates that within the BLA GAD− neurons, a subpopulation is activated by withdrawal in terms of c-*fos* mRNA, whereas another is inhibited. The number of c-*fos*+/GAD+ neurons (Fig. 4B) was not significantly altered in any situation (n = 109 for the Nal120 group vs n = 87 for the Sal group), but the median of grain density (Fig. 4B, inset) was also increased after acute withdrawal to reach 49.9 versus 13.6 in the Sal group, indicating a global increase in the activity of this cell population.

c-*fos* responses in phenotypic identified neurons of the VTA

Double-labeling showed that acute withdrawal (Fig. 2E) increased the density of c-*fos*+/TH+ (+325%) as well as c-*fos*+/TH− (+544%) neurons. These data were confirmed by c-*fos*/GAD67 mRNA double labeling, showing that c-*fos*+/GAD+ neurons matched c-*fos*+/TH− neurons (data not shown). Reexposure to withdrawal-paired stimuli (Fig. 2F) also induced c-*fos* expression in both TH+ (+309% for ENV+/cs+, +315% for ENV+/cs−) and TH− (+265% for ENV+/cs+, +296% for ENV+/cs−) neurons. If we consider the total number of c-*fos*+ neurons in each group, ~50% were TH+ and 50% were TH− (Fig. 2E,F). However, in the VTA, the density of dopamine (DA) neurons (TH+) is an average 4.5-fold higher than the number of GABA (GAD+) neurons (mean ± SEM: 373 ± 10 per mm^2 for TH+ and 83 ± 3 per mm^2 for GAD+ overall). Thus, our data showed that most GAD+ neurons expressed c-*fos* after both acute withdrawal (80 ± 8% for Nal120) and reexposure to withdrawal-paired stimuli (65 ± 9% for ENV+/cs+, 67 ± 8% for ENV+/cs−). In addition, we clearly demonstrated here that a small but significant proportion of the TH+ population showed
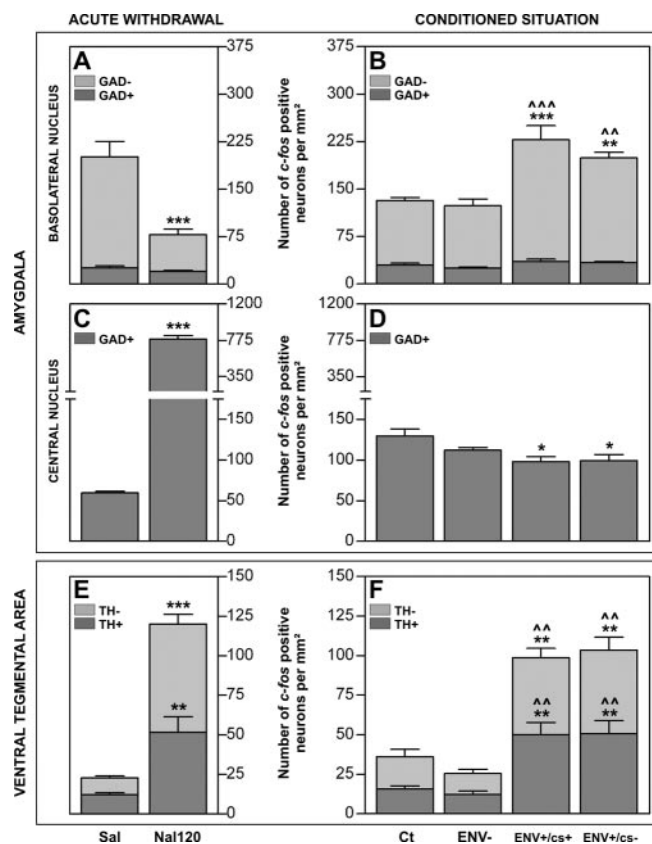

Figure 2. c-*fos* mRNA expression in phenotypically identified neurons of the BLA (A, B), CeA (C, D), and VTA (E, F) after acute withdrawal (A, C, E) and reexposure to withdrawal-paired stimuli (conditioned situation; B, D, F) is shown. A, B, E, F, Stacked histograms representing mean ± SEM of the density of c-*fos*+ neurons per millimeter squared in GAD+ (dark bars) and GAD− (light bars) BLA neurons (A, B) and in TH+ (dark bars) and TH− (light bars) VTA neurons (E, F). The total number of c-*fos*+ neurons in each group is represented by the entire bar (dark plus light bars). In the BLA, c-*fos*+ neurons were decreased in GAD− neurons after acute withdrawal (A; Nal120 group) (unpaired t test; ***p < 0.001 vs Sal group) but, in contrast, increased after reexposure to withdrawal-associated stimuli (B; ENV+/cs+ and ENV+/cs− groups) (ANOVA: p < 0.0001; post hoc Newman–Keuls test: **p < 0.01, ***p < 0.001 vs Ct group; ^^p < 0.01, ^^^p < 0.001 vs ENV− group). In contrast, c-*fos*+/GAD+ neurons in the BLA were not significantly different in both situations. In the VTA, c-*fos* mRNA was increased in both TH+ and TH− neurons after either acute withdrawal (E; Nal120 group) (unpaired t test; **p < 0.01 vs Sal group for c-*fos*+/TH+; ***p < 0.0001 vs Sal group for c-*fos*+/TH−) or reexposure to withdrawal-paired stimuli (F; ENV+/cs+ and ENV+/cs− groups) (ANOVA: p < 0.0003 for c-*fos*+/TH+, p < 0.0003 for c-*fos*+/TH−; post hoc Newman–Keuls test: **p < 0.01 vs Ct group, ^^p < 0.01 vs ENV− group). The withdrawal-induced and conditioned increases in c-*fos* neurons were similar in TH+ and TH− VTA neurons, representing approximately half of the total c-*fos*+ neurons. C, D, Bars represent mean ± SEM of c-*fos*+ neurons per millimeter squared in CeA GAD+ neurons. The number of double-labeled neurons was strongly increased after acute withdrawal (E; Nal120 group) (unpaired t test; ***p = 0.0001 vs Sal group) but decreased after reexposure to withdrawal-paired stimuli (F; ENV+/cs+ and ENV+/cs− groups) (ANOVA: p = 0.0117; post hoc Newman–Keuls test, *p < 0.05 vs Ct group). There was no significant difference in c-*fos* expression between ENV+/cs+ and ENV+/cs− animals in the various neuronal populations of the BLA, CeA, and VTA.

c-*fos* mRNA inductions both in the acute (13 ± 2% for Nal120) and conditioned (14 ± 2% for ENV+/cs+, 13 ± 2% for ENV+/cs−) situations.

Discussion

Dissociations in the neural pathways mediating withdrawal memories and acute withdrawal

We show here that reexposure to a withdrawal-paired environment specifically induces conditioned c-*fos* responses in the extended amygdala [CeA, bed nucleus of the stria terminalis
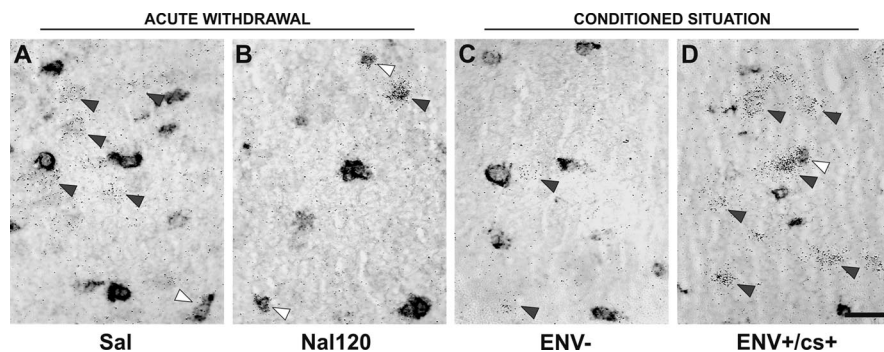
ACUTE WITHDRAWAL　　　　**CONDITIONED SITUATION**

Sal　　　　Nal120　　　　ENV-　　　　ENV+/cs+

Figure 3. Photomicrographs illustrating the opposite patterns of c-fos mRNA expression detected in phenotypically identified neurons of the BLA after either acute naloxone-precipitated morphine withdrawal (A, B) or reexposure to an environment previously paired with withdrawal (C, D). Double in situ hybridization detects GAD67 mRNA with digoxigenin-labeled riboprobe (stained cells), together with c-fos mRNA with a ^{35}S-labeled riboprobe (silver grains). Gray stained cells correspond to the GABAergic interneurons of the BLA. White arrowheads point to double-labeled neurons for c-fos and GAD67 mRNAs, and gray arrowheads point to single-labeled neurons for c-fos mRNA, which correspond to the glutamatergic efferents of the BLA. In the Sal group (A), many GAD− neurons expressed c-fos mRNA, whereas few GAD+ neurons exhibited c-fos labeling. The basal levels of c-fos mRNA expression per neuron (silver grain density) were relatively low in both GAD+ and GAD− neurons (A). The density of c-fos+ neurons was much lower in ENV− animals (compared with the Sal group), and sparse GAD− neurons exhibited c-fos labeling (C). After naloxone-precipitated morphine withdrawal using 120 μg/kg (B), the density of c-fos+/GAD− neurons was clearly decreased, but interestingly, the remaining c-fos-labeled neurons displayed a higher density of silver grains (gray arrowhead in B) compared with the control situation (gray arrowhead in A). In contrast, reexposure to withdrawal-paired stimuli increased both the density of c-fos+/GAD− neurons (D) and the number of silver grains per neuron compared with ENV− animals (C), showing a classical increase in global c-fos activity. Scale bar, 50 μm.

(BNST), and accumbens nucleus (Acb)] as well as in the VTA, hippocampus, BLA, LC, and hypothalamus. All of these structures are involved in opiate addiction and various processes occurring during withdrawal. Interestingly, we have already shown that, when opiate withdrawal is precipitated by naloxone doses that only induce an aversive state without somatic signs, c-fos mRNA responses also occurred specifically in the extended amygdala, VTA, hippocampus, and BLA (Frenois et al., 2002), suggesting that this limbic circuit could specifically mediate the affective value of withdrawal-paired stimuli. The shell medial part of the Acb, BNST, and CeA are highly interconnected limbic areas that represent the main components of the extended amygdala, and our data strongly support the idea that they represent critical components for mediating incentive-learning processes (Aston-Jones et al., 1999; Koob, 1999; De Vries and Shippenberg, 2002; Everitt et al., 2003) and are also consistent with the proposed key role of the ventral part of the BNST in the aversive component of opiate withdrawal (Delfs et al., 2000). Our data also suggest that the LC and the hypothalamus may be involved in the retrieval and/or expression of aversive learned associations, contrasting with the common idea excluding the LC from the motivational component of withdrawal (Caillé et al., 1999; Delfs et al., 2000; Frenois et al., 2002). However, the LC together with several hypothalamic nuclei are also essential in mediating anxiety, stress responses, and/or arousal (Aston-Jones et al., 1999; Koob, 1999), which fully participate to the emotional component of withdrawal and its memory, especially in our experimental condition.

Interestingly, our conditioned c-fos responses were identical in rats reexposed to the cs+ or cs− compartments (ENV+) but not in rats with the same history of withdrawal in another context (ENV−). This occurs despite the fact that during the aversion test ENV+ rats avoided the cs+ compartment, indicating that they have efficiently associated the cs+ compartment features with the aversive experience of withdrawal. This indicates a conditioning to the context that is neurochemically expressed in terms of c-fos

expression when rats are confined in a Y-maze compartment in which they are no longer able to compare the features of each compartment. One explanation would be that when confined, the affective state of the animals is more under the control of distal contextual cues, whereas when given the choice, animals may additionally use the set of proximal stimuli to direct their behavior in the Y-maze. Additional experiments are required to understand how the limbic structures identified here are involved in the emotional versus cognitive influences of withdrawal memories on behavioral outcomes.

We also show that the neural correlates of withdrawal memories and acute opiate withdrawal are partially dissociated because conditioned c-fos responses occur in structures representing only a subset of the many areas recruited by naloxone-precipitated withdrawal (Frenois et al., 2002). More interestingly, a double dissociation was found within the amygdala, suggesting that the acute and conditioned withdrawal effects are differentially coded in the CeA and BLA. Together, our data reveal anatomical and functional dissociations in the processes involved in the incentive–motivational properties of withdrawal-paired stimuli and of acute opiate withdrawal. This correlates well with studies performed on animal models of relapse, analyzing the conditioned and acute appetitive properties of drugs (Self and Nestler, 1998; See, 2002; Shalev et al., 2002). c-Fos expression and local transitory inactivation procedures have also found partial dissociations between the circuits underlying the effects of drug-paired stimuli and those involved in drug reinforcement/reinstatement (Brown et al., 1992; Grimm and See, 2000; Neisewander et al., 2000). This contrasts with the view that drug-paired stimuli can reinstate drug seeking by engaging neural processes similar to those recruited by the drug itself (Stewart et al., 1984).

Functional consequences for the formation and retrieval of withdrawal memories
The architecture of the extended amygdala (Alheid and Heimer, 1988; Schmued, 1994; Cardinal et al., 2002) and its modulation by DA inputs (Phelix et al., 1992; Freedman and Cassell, 1994) strongly supports the processing of emotional events in relation with environmental stimuli to set off motivated behaviors (Cardinal et al., 2002). Imaging data also support the idea that this network is critical to mediate the incentive–motivational properties of withdrawal (Gracy et al., 2001; Frenois et al., 2002). Interestingly, in our model, the c-fos responses of acute withdrawal were measured after the first conditioning session. In the amygdala, which is involved in memory processing and pavlovian conditioning, the c-fos responses might therefore sustain the onset of associative learning processes to encode the incentive value of withdrawal-paired stimuli. Indeed, conditioned place aversion can be induced by one pairing (Stinus et al., 1990), indicating that the first withdrawal syndrome is sufficient for the formation of an association between the withdrawal aversive state and the environment. Conversely, reexposure of conditioned animals to withdrawal-paired stimuli reflects the retrieval of the learned associations.
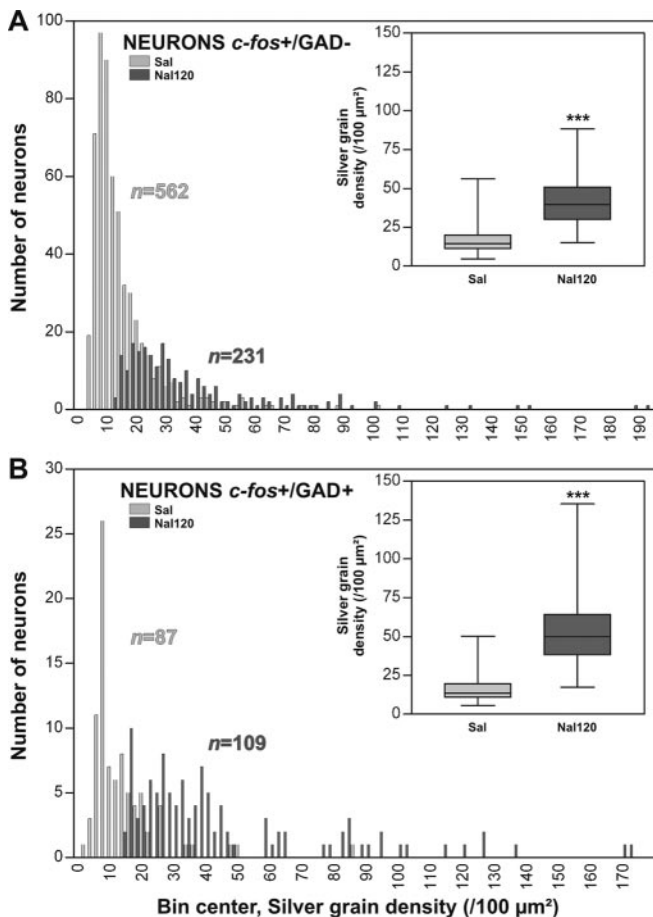
Figure 4. In the BLA, frequency distributions of grain densities in c-fos+/GAD− (*A*) and c-fos+/GAD+ (*B*) neurons after acute withdrawal (dark histogram) compared with control (light histogram) are shown. Insets, box-plots showing the medians (middle line of the box), 25th and 75th percentiles (base and top of the box), and minimal/maximal values for both groups (Sal, light box; Nal120, dark box). For GAD− neurons (*A*), 562 neurons showed c-fos labeling in controls (light histogram), whereas c-fos+ neurons decreased after acute withdrawal ($n = 231$; dark histogram). However, the median of grain density (inset in *A*) was increased after acute withdrawal (Nal120 group) to reach 39.6 (25th and 75th percentiles = 30.2 and 50.7, respectively) compared with 14.6 (25th and 75th percentiles = 11.4 and 19.9, respectively) in the Sal group (Mann–Whitney test; ***$p < 0.0001$). For the GAD+ population (*B*), c-fos+ neurons were not significantly altered after acute withdrawal ($n = 109$; dark histogram) compared with controls ($n = 87$; light histogram). However, the median of silver grain density (inset in *B*) was increased after acute withdrawal (Nal120 group) to reach 49.9 (25th and 75th percentiles = 38.2 and 64.2, respectively) compared with 13.6 (25th and 75th percentiles = 10.8 and 19.6, respectively) in the Sal group (Mann–Whitney test; ***$p < 0.0001$). The Kolmogorov–Smirnov test showed significant differences between the frequency distributions in the Sal and Nal120 groups for both neuronal populations ($\chi^2 = 270.01$ for c-fos+/GAD+; $\chi^2 = 97.764$ for c-fos+/GAD−; $p < 0.0001$ in both cases).

Differential involvement of BLA and CeA neurons
The BLA contains GABA interneurons modulating glutamate output neurons (Pitkanen et al., 1997). In the BLA, we showed that, if the number of c-fos+ neurons was decreased in the glutamate (GAD−) population after the first conditioning session, c-fos expression in the remaining labeled neurons was clearly increased. In addition, the c-fos mRNA level in GABA neurons was also increased. Thus, BLA neuronal activity is not globally decreased during withdrawal, and our data suggest that a BLA output subpopulation is facilitated, whereas another is inhibited during conditioning. Furthermore, this could explain that retrieval of withdrawal memories also enhanced c-fos expression specifically in glutamatergic neurons. The CeA is the main

GABAergic output nucleus of the amygdala and receives sensory glutamatergic inputs from the BLA (Cassell et al., 1999). Moreover, the intercalated cells (ITCs) interposed between the BLA and CeA (Millhouse, 1986; Cassell et al., 1999) generate feedforward inhibition in CeA neurons (Royer et al., 1999; Pare et al., 2003). As in the BLA, we show opposite c-fos responses in the CeA with a strong increase after acute withdrawal but a decrease after reexposure to withdrawal-paired stimuli. Because the c-fos responses detected in the CeA are opposite of those obtained in the BLA in these two situations (double dissociation), they might in part be attributable to changes in BLA efferent activity via the ITC.

Differential involvement of VTA neurons
Most VTA GABA neurons showed enhanced c-fos expression after both acute withdrawal and reexposure to withdrawal-paired stimuli, reflecting an activation of these interneurons that would drive DA neuron inhibition, as expected from Bonci and Williams (1997). Interestingly, we show here that a subpopulation of VTA DA neurons is activated after acute withdrawal and reexposure to withdrawal-paired stimuli (13–14% of DA neurons). This original result shows that opposite responses within subpopulations of DA neurons could mediate both the formation and retrieval of withdrawal memories. The weak proportion of these neurons, along with consistent global-reduced activity of VTA DA neurons and decreased DA release in the Acb during withdrawal (Acquas and Di Chiara, 1992; Rossetti et al., 1992; Georges and Aston-Jones, 2003) leads to the hypothesis that DA neurons activated during withdrawal project to other structures than the Acb, including the BLA (Freedman and Cassell, 1994; Brinley-Reed and McDonald, 1999). This question is currently under detailed investigation, with the hypothesis that DA activity in the amygdala during withdrawal may participate in the association between opiate withdrawal and environmental stimuli. This effect would be sensitized by the repeated conditioning sessions, allowing a potentiated DA modulation on BLA outputs. This hypothesis is in line with data using other models showing that increased DA activity in the amygdala is critical for mediating aversive conditioning (Coco et al., 1992; Guarraci et al., 1999; Nader and Le Doux, 1999).

Functional outcomes
Retrieval of aversive learned associations are modulated by VTA-amygdaloid projections through DA-mediated processes (Nader and Le Doux, 1999), and DA modulates neuronal plasticity in the BLA during associative learning (Rosenkranz and Grace, 2002b; Bissiere et al., 2003). Accordingly, we show here that withdrawal-paired stimuli induced variations of c-fos expression in the VTA and its projection territories (Acb and BLA). Therefore, we suggest that the retrieval of aversive learned associations is processed via DA interactions in the BLA, enhancing the activity of BLA glutamatergic outputs, which *in fine* could drive drug-seeking motivation through changes in output structures. In several elegant studies, Rosenkranz and Grace (1999, 2001, 2002a) described the mechanisms by which DA may enhance the signal/noise ratios over a subpopulation of BLA efferents, allowing sensory inputs to drive BLA outputs. Our complex c-fos responses in the BLA during the first conditioning session could reflect such a gating mechanism, by which influence of sensory inputs could be facilitated in a subpopulation of BLA outputs. This gating process could be sensitized through repetition of the conditioning sessions and explain why reexposure to withdrawal-paired stimuli induces a conditioned increase in c-fos expression

specifically within many BLA output neurons that might have increased in number across the conditioning sessions.

We propose that c-*fos* variations after acute withdrawal in a specific environment could reflect the onset of associative learning processes aimed to encode the incentive value of the withdrawal-paired environment in the acute situation (memory formation). Conversely, reexposure to withdrawal-paired environmental stimuli would reflect the expression of learned associations in the conditioned situation (memory retrieval). This is currently under detailed investigation.

Conclusion

Addiction can be viewed as a chronically relapsing disorder, with the involvement of motivational, emotional, and memory-related processes (Everitt et al., 1999; Robinson and Berridge, 2000). With the recent increasing evidence that the negative affective state of opiate withdrawal could enhance the incentive value of the drug and contribute to the maintenance of drug-seeking behavior (Ahmed et al., 2000; Hutcheson et al., 2001), our data represent one critical step in the understanding of these processes. Our work will then contribute to understand how specific environments associated with opiate withdrawal might drive drug-seeking motivation.

References

Acquas E, Di Chiara G (1992) Depression of mesolimbic dopamine transmission and sensitization to morphine during opiate abstinence. J Neurochem 58:1620–1625.

Ahmed SH, Walker JR, Koob GF (2000) Persistent increase in the motivation to take heroin in rats with a history of drug escalation. Neuropsychopharmacology 22:413–421.

Alheid GF, Heimer L (1988) New perspectives in basal forebrain organization of special relevance for neuropsychiatric disorders: the striatopallidal, amygdaloid, and corticopetal components of substantia innominata. Neuroscience 27:1–39.

Aston-Jones G, Rajkowski J, Cohen J (1999) Role of locus coeruleus in attention and behavioral flexibility. Biol Psychiatry 46:1309–1320.

Bissiere S, Humeau Y, Luthi A (2003) Dopamine gates LTP induction in lateral amygdala by suppressing feedforward inhibition. Nat Neurosci 6:587–592.

Bonci A, Williams JT (1997) Increased probability of GABA release during withdrawal from morphine. J Neurosci 17:796–803.

Brinley-Reed M, McDonald AJ (1999) Evidence that dopaminergic axons provide a dense innervation of specific neuronal subpopulations in the rat basolateral amygdala. Brain Res 850:127–135.

Brown EE, Robertson GS, Fibiger HC (1992) Evidence for conditional neuronal activation following exposure to a cocaine-paired environment: role of forebrain limbic structures. J Neurosci 12:4112–4121.

Caillé S, Espejo EF, Reneric JP, Cador M, Koob GF, Stinus L (1999) Total neurochemical lesion of noradrenergic neurons of the locus coeruleus does not alter either naloxone-precipitated or spontaneous opiate withdrawal nor does it influence ability of clonidine to reverse opiate withdrawal. J Pharmacol Exp Ther 290:881–892.

Cardinal RN, Parkinson JA, Hall J, Everitt BJ (2002) Emotion and motivation: the role of the amygdala, ventral striatum, and prefrontal cortex. Neurosci Biobehav Rev 26:321–352.

Cassell MD, Freedman LJ, Shi C (1999) The intrinsic organization of the central extended amygdala. Ann NY Acad Sci 877:217–241.

Childress AR, Hole AV, Ehrman RN, Robbins SJ, McLellan AT, O'Brien CP (1993) Cue reactivity and cue reactivity interventions in drug dependence. NIDA Res Monogr 137:73–95.

Coco ML, Kuhn CM, Ely TD, Kilts CD (1992) Selective activation of mesoamygdaloid dopamine neurons by conditioned stress: attenuation by diazepam. Brain Res 590:39–47.

Curran T, Gordon MB, Rubino KL, Sambucetti LC (1987) Isolation and characterization of the c-fos(rat) cDNA and analysis of post-translational modification in vitro. Oncogene 2:79–84.

Delfs JM, Zhu Y, Druhan JP, Aston-Jones G (2000) Noradrenaline in the

ventral forebrain is critical for opiate withdrawal-induced aversion. Nature 403:430–434.

De Vries TJ, Shippenberg TS (2002) Neural systems underlying opiate addiction. J Neurosci 22:3321–3325.

Everitt BJ, Parkinson JA, Olmstead MC, Arroyo M, Robledo P, Robbins TW (1999) Associative processes in addiction and reward. The role of amygdala-ventral striatal subsystems. Ann NY Acad Sci 877:412–438.

Everitt BJ, Cardinal RN, Parkinson JA, Robbins TW (2003) Appetitive behavior: impact of amygdala-dependent mechanisms of emotional learning. Ann NY Acad Sci 985:233–250.

Freedman LJ, Cassell MD (1994) Distribution of dopaminergic fibers in the central division of the extended amygdala of the rat. Brain Res 633:243–252.

Frenois F, Cador M, Caillé S, Stinus L, Le Moine C (2002) Neural correlates of the motivational and somatic components of naloxone-precipitated morphine withdrawal. Eur J Neurosci 16:1377–1389.

Georges F, Aston-Jones G (2003) Prolonged activation of mesolimbic dopaminergic neurons by morphine withdrawal following clonidine: participation of imidazoline and norepinephrine receptors. Neuropsychopharmacology 28:1140–1149.

Gestreau C, Le Guen S, Besson JM (2000) Is there tonic activity in the endogenous opioid systems? A c-Fos study in the rat central nervous system after intravenous injection of naloxone or naloxone-methiodide. J Comp Neurol 427:285–301.

Gold LH, Stinus L, Inturrisi CE, Koob GF (1994) Prolonged tolerance, dependence and abstinence following subcutaneous morphine pellet implantation in the rat. Eur J Pharmacol 253:45–51.

Gracy KN, Dankiewicz LA, Koob GF (2001) Opiate withdrawal-induced fos immunoreactivity in the rat extended amygdala parallels the development of conditioned place aversion. Neuropsychopharmacology 24:152–160.

Grimm JW, See RE (2000) Dissociation of primary and secondary reward-relevant limbic nuclei in an animal model of relapse. Neuropsychopharmacology 22:473–479.

Guarraci FA, Frohardt RJ, Young SL, Kapp BS (1999) A functional role for dopamine transmission in the amygdala during conditioned fear. Ann NY Acad Sci 877:732–736.

Hamlin A, Buller KM, Day TA, Osborne PB (2001) Peripheral withdrawal recruits distinct central nuclei in morphine-dependent rats. Neuropharmacology 41:574–581.

Hutcheson DM, Everitt BJ, Robbins TW, Dickinson A (2001) The role of withdrawal in heroin addiction: enhances reward or promotes avoidance? Nat Neurosci 4:943–947.

Julien JF, Legay F, Dumas S, Tappaz M, Mallet J (1987) Molecular cloning, expression and in situ hybridization of rat brain glutamic acid decarboxylase messenger RNA. Neurosci Lett 73:173–180.

Koob GF (1999) Corticotropin-releasing factor, norepinephrine, and stress. Biol Psychiatry 46:1167–1180.

Koob GF, Le Moal M (2001) Drug addiction, dysregulation of reward, and allostasis. Neuropsychopharmacology 24:97–129.

Millhouse OE (1986) The intercalated cells of the amygdala. J Comp Neurol 247:246–271.

Nader K, Le Doux JE (1999) Inhibition of the mesoamygdala dopaminergic pathway impairs the retrieval of conditioned fear associations. Behav Neurosci 113:891–901.

Neisewander JL, Baker DA, Fuchs RA, Tran-Nguyen LT, Palmer A, Marshall JF (2000) Fos protein expression and cocaine-seeking behavior in rats after exposure to a cocaine self-administration environment. J Neurosci 20:798–805.

Pare D, Royer S, Smith Y, Lang EJ (2003) Contextual inhibitory gating of impulse traffic in the intra-amygdaloid network. Ann NY Acad Sci 985:78–91.

Paxinos G, Watson C (1997) The rat brain in stereotaxic coordinates, Ed 3. San Diego: Academic.

Phelix CF, Liposits Z, Paull WK (1992) Monoamine innervation of bed nucleus of stria terminalis: an electron microscopic investigation. Brain Res Bull 28:949–965.

Pitkanen A, Savander V, Le Doux JE (1997) Organization of intra-amygdaloid circuitries in the rat: an emerging framework for understanding functions of the amygdala. Trends Neurosci 20:517–523.

Robinson TE, Berridge KC (2000) The psychology and neurobiology of addiction: an incentive-sensitization view. Addiction 95 [Suppl 2]:S91–S117.

Rosenkranz JA, Grace AA (1999) Modulation of basolateral amygdala neu-

ronal firing and afferent drive by dopamine receptor activation *in vivo*. J Neurosci 19:11027–11039.

Rosenkranz JA, Grace AA (2001) Dopamine attenuates prefrontal cortical suppression of sensory inputs to the basolateral amygdala of rats. J Neurosci 21:4090 – 4103.

Rosenkranz JA, Grace AA (2002a) Cellular mechanisms of infralimbic and prelimbic prefrontal cortical inhibition and dopaminergic modulation of basolateral amygdala neurons *in vivo*. J Neurosci 22:324 –337.

Rosenkranz JA, Grace AA (2002b) Dopamine-mediated modulation of odour-evoked amygdala potentials during pavlovian conditioning. Nature 417:282–287.

Rossetti ZL, Hmaidan Y, Gessa GL (1992) Marked inhibition of mesolimbic dopamine release: a common feature of ethanol, morphine, cocaine and amphetamine abstinence in rats. Eur J Pharmacol 221:227–234.

Royer S, Martina M, Pare D (1999) An inhibitory interface gates impulse traffic between the input and output stations of the amygdala. J Neurosci 19:10575–10583.

Schmued LC (1994) Diagonal ventral forebrain continuum has overlapping telencephalic inputs and brainstem outputs which may represent loci for limbic/autonomic integration. Brain Res 667:175–191.

Schulteis G, Markou A, Gold LH, Stinus L, Koob GF (1994) Relative sensi-

tivity to naloxone of multiple indices of opiate withdrawal: a quantitative dose-response analysis. J Pharmacol Exp Ther 271:1391–1398.

See RE (2002) Neural substrates of conditioned-cued relapse to drug-seeking behavior. Pharmacol Biochem Behav 71:517–529.

Self DW, Nestler EJ (1998) Relapse to drug-seeking: neural and molecular mechanisms. Drug Alcohol Depend 51:49 – 60.

Shalev U, Grimm JW, Shaham Y (2002) Neurobiology of relapse to heroin and cocaine seeking: a review. Pharmacol Rev 54:1– 42.

Stewart J, de Wit H, Eikelboom R (1984) Role of unconditioned and conditioned drug effects in the self-administration of opiates and stimulants. Psychol Rev 91:251–268.

Stinus L, Le Moal M, Koob GF (1990) Nucleus accumbens and amygdala are possible substrates for the aversive stimulus effects of opiate withdrawal. Neuroscience 37:767–773.

Svenningsson P, Fredholm BB, Bloch B, Le Moine C (2000) Co-stimulation of D(1)/D(5) and D(2) dopamine receptors leads to an increase in c-fos messenger RNA in cholinergic interneurons and a redistribution of c-fos messenger RNA in striatal projection neurons. Neuroscience 98:749–757.

Wikler A (1973) Dynamics of drug dependence. Implications of a conditioning theory for research and treatment. Arch Gen Psychiatry 28:611– 616.